Weissmueller, J.; Markmann, J.; Grewer, M.; Birringer, R.:
Kinematics of polycrystal deformation by grain boundary sliding
In: Acta Materialia (2011) Elsevier

DOI: 10.1016/j.actamat.2011.03.060

Kinematics of Polycrystal Deformation by Grain Boundary Sliding

Jörg Weissmüller and Jürgen Markmann
Institut für Werkstoffphysik und -Technologie, Technische Universität Hamburg-Harburg, Hamburg, Germany and Institut für Werkstofmechanik, Helmholtz-Zentrum Geesthacht, Geesthacht, Germany

Manuel Grewer and Rainer Birringer
Technische Physik, Universität dess Saarlandes, Saarbrücken, Germany

We analyze the macroscopic deformation of a polycrystalline solid due to local deformation events in the core of grain boundaries. The central result is an equation that decomposes the effective macroscopic strain into contributions from three deformation modes, namely *i*) the elastic strain in the bulk of the crystallites, *ii*) the results of dislocation glide and climb processes, and *iii*) the deformation of events in the grain boundary core. The latter process is represented by jumps in the displacement vector field that can be decomposed into tangential ('slip') and normal ('stretch') components. The relevant measure for the grain-boundary mediated deformation is not the displacement jump vector but a grain boundary discontinuity tensor that depends on the displacement jump and on the orientation of the grain boundary normal. Accommodation processes at triple junctions do not contribute significantly to the macroscopic strain. By means of example, the theory is applied to the effective elastic response of nanocrystalline materials with an excess slip compliance at grain boundaries. The predictions, specifically on the size-dependence of the Poisson ratio, agree with recent experiments on nanocrystalline Pd. The value of the slip compliance for grain boundaries in Pd is obtained as 18pm/GPa.

I. INTRODUCTION

It is widely accepted that the mechanisms of plastic deformation of materials with a nanoscale grain size differ from those of conventional, coarse-grained polycrystals [1–3]. Since the stress which is required to activate dislocation plasticity increases with decreasing grain size, one may suspect that dislocation glide or climb becomes marginal in the limit of very small grains. Conversely, the abundance of grain boundaries in nanocrystalline materials suggest that local deformation events in the core of grain boundaries evolve as a relevant deformation mechanism.

Indeed, the signatures of grain boundary sliding and grain rotation have been identified in experiment and in atomistic simulation. The lack of deformation texture in nanocrystalline metals testifies to grain rotation promoted by sliding [4], and that same process is directly observed in computer simulation [5, 6]. Furthermore, recent experiments point towards an elastic shear softening of grain boundary regions [7], again in agreement with atomistic simulation [8–10]. The finding suggests that boundaries may deform elastically by shear in their tangent plane. This deformation mode would be the equivalent to grain boundary sliding, yet it involves the regime of elastic instead of plastic deformation. Besides simple grain boundary sliding, recent research highlights the coupling between tangential shear and grain boundary migration [11, 12]. This 'coupled motion' is apparent in experiments with bicrystals [13, 14] and has also been identified in atomistic studies of nanocrystal deformation [15, 16].

While there is ample evidence for the presence of grain boundary sliding in nanocrystalline material deformation, dislocation plasticity is widely recognized to remain a relevant contribution, at the very least in its property as an accommodation process for grain-boundary mediated processes. In fact, experimental evidence for dislocation generation and twinning [17–19] is in good agreement with direct observation of dislocation nucleation and glide in computer simulation [20].

The state of the art is thus that the plasticity of nanocrystalline metals involves local deformation events at grain boundaries along with lattice dislocation activity. In the elastic regime at small stress, an excess of compliance, possibly in shear, may contribute to the effective macroscopic response to load along with the conventional bulk elastic deformation. These observations suggest the obvious question, how can the relative contributions of the bulk- and grain boundary processes to the overall deformation be quantified?

Studies using atomistic simulation have analyzed separately the deformation due to dislocation plasticity and the total macroscopic deformation, finding large differences that points towards a significant contribution of grain-boundary sliding [6, 21]. Yet, a direct and quantitative investigation of the role of sliding has not been forthcoming for lack of a kinematic theory linking local sliding and macroscopic strain. Here, we derive this theory.

Figure 1 is a schematic illustration of grain boundary mediated deformation of a polycrystal for the example of shearing. In an idealized brick-wall microstructure – made out of identical rectangular grains of size L (top row in the figure) – a conceivable deformation mode involves uniform slip by the distance τ along sets of coplanar boundaries. This would result in a net macroscopic shear in the order of τ/L. Yet, the analogous process in a realistic polycrystalline microstructure (bottom row in Fig. 1) is more complex. It is liable to involve nonuniform

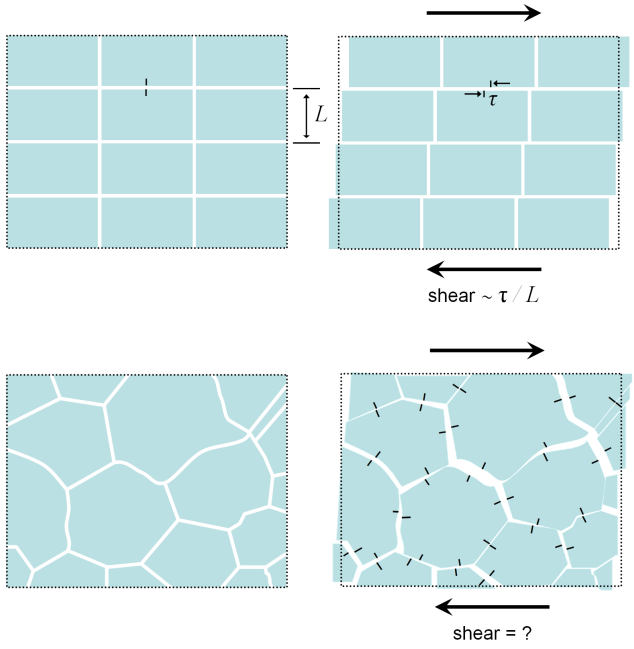

FIG. 1. Schematic illustration of polycrystal deformation mediated by grain boundary processes. Top row shows shear by grain boundary sliding or shear in an idealized brick model of a polycrystal. The macroscopic shear is in the order of slip distance, τ, over grain size, L. Bottom row shows realistic polycrystalline microstructure. Grain boundary deformation may be tangential as well as perpendicular to the boundary plane. These events occur on boundaries oriented at arbitrary angles to the macroscopic shear stress or strain. Furthermore, stress concentrations – for instance at triple lines – call for accommodation by elastic or plastic bulk deformation. It is then not obvious how the local deformation events relate to the macroscopic strain. Lines across grain boundaries are markers showing local slip.

slip on boundaries oriented at arbitrary angles relative to the macroscopic stress or strain direction, along with possible out-of-plane deformation modes. Furthermore, incompatibilities at triple lines require accommodation by elastic or plastic deformation of the bulk. Given this general deformation mode, the questions at hand are twofold. First, what is a suitable measure for the local deformation at a grain boundary? Second, if the values of this deformation variable are known everywhere on the grain boundary network along with the complete information on bulk strain as well as bulk dislocation movement, how can one compute the macroscopic strain?

Our analysis of the above issues starts out with considerations (in Section 2) on the kinematics of grain boundary deformation. We then investigate the roles of elastic accommodation (Section 3) and of dislocation plasticity in the bulk (Section 4). In order to illustrate the application of our theory to experiment, we inspect (Section 5) a toy model for interfacial excess elasticity that can be compared to experimental data [7] for the effective elastic behavior of nanocrystalline Pd.

II. KINEMATICS

A. Geometry and definitions

We consider a polycrystalline solid body B (Figure 2) consisting of a space-filling array of crystallites (grains) C_j. We take B to be bounded by the external surface S, and we denote the internal interfaces (grain boundaries) between grains j and k by G_{jk}. We adopt a small-strain continuum description in which the deformation relative to a reference configuration is embodied in a displacement vector field $\mathbf{u}(\mathbf{r})$ where $\mathbf{r}$ is a position vector in B. The macroscopic deformation is represented by the displacements on the external surface, which we denote by $\mathbf{u}_\mathsf{S}(\mathbf{r}_\mathsf{S})$. The subscript denotes values defined on S. The

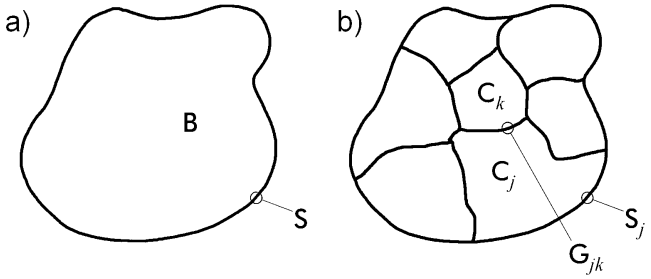

FIG. 2. Part a), schematic illustration of the body B with external surface S. Part b) illustrates grain structure and notation for external surface, S_j, of grain j and grain boundary G_{jk} joining grains j and k.

location of the interfaces is considered stationary in reference coordinates; this excludes grain boundary migration from our analysis.

Let us start out by taking $\mathbf{u}(\mathbf{r})$ was a *continuous* displacement field. Then $\mathbf{u}_\mathsf{S}$ is related to the displacement gradient–as represented by the second rank tensor $\nabla\mathbf{u}$–in the bulk via the divergence law [22]

$$\int_\mathsf{S} \mathbf{u}_\mathsf{S} \otimes \mathbf{n} \mathrm{d}A = \int_\mathsf{B} \nabla\mathbf{u} \mathrm{d}V \ , \tag{1}$$

where $\mathbf{n}(\mathbf{r}_\mathsf{S})$ represents the outer surface normal and $\otimes$ refers to the Kronecker product (see Appendix for tensor notation). Even though we allow for quantities such as $\mathbf{n}$, $\mathbf{u}$, $\nabla\mathbf{u}$ to depend on position, we suppress the display of the position variable in the equations for brevity.

The antisymmetric part of Equation (1) represents a rigid body rotation which does not involve strain. We will here focus on the symmetric part,

$$\frac{1}{2}\int_\mathsf{S} (\mathbf{u}_\mathsf{S} \otimes \mathbf{n} + \mathbf{n} \otimes \mathbf{u}_\mathsf{S}) \, \mathrm{d}A = \int_\mathsf{B} \mathbf{E} \mathrm{d}V \ , \tag{2}$$

where $\mathbf{E}$ denotes the strain, $\mathbf{E} = \frac{1}{2}(\nabla\mathbf{u} + \nabla\mathbf{u}^\mathrm{T})$ with the superscript 'T' denoting transposition. The left-hand side

of Eq. (2) defines an effective macroscopic strain tensor, $\mathbf{E}_{\text{eff}}$, via

$$\mathbf{E}_{\text{eff}} = \frac{1}{2V}\int_{\mathsf{S}} (\mathbf{u}_{\mathsf{S}} \otimes \mathbf{n} + \mathbf{n} \otimes \mathbf{u}_{\mathsf{S}})\, \mathrm{d}A \,. \tag{3}$$

When the deformation is continuous in the bulk, then Eq. (2) shows that $\mathbf{E}_{\text{eff}}$ as measured by the surface displacements agrees with the volume-average of the strain $\mathbf{E}$ in the bulk.

B. Displacement jump

Let us now allow for discontinuity of the displacement at grain boundaries. We shall initially ignore dislocation activity, so that $\mathbf{u}(\mathbf{r})$ remains continuous *within* each grain. Equation (1) can then be applied separately to each grain j:

$$\sum_k \int_{\mathsf{G}_{jk}} \mathbf{u}_{\mathsf{G}_{jk}} \otimes \mathbf{n}_{jk} \mathrm{d}A + \int_{\mathsf{S}_j} \mathbf{u}_{\mathsf{S}_j} \otimes \mathbf{n}_j \mathrm{d}A = \int_{\mathsf{C}_j} \nabla \mathbf{u} \mathrm{d}V \,. \tag{4}$$

The terms on the left-hand side account for the displacements, $\mathbf{u}_{\mathsf{G}_{jk}}$ and $\mathbf{u}_{\mathsf{S}_j}$, along the individual grain boundaries G_{jk} with the neighboring grains k as well as–where applicable–the displacements on an intersection, S_j, of the grain with the external surface. Figure 3 illustrates the definition of $\mathbf{u}_{\mathsf{G}_{jk}}$ as the limiting value of $\mathbf{u}$ as the boundary between grains j and k is approached from within grain j.

In Eq. (4), the $\mathbf{n}_{jk}$ represent the outer normal of the grain boundary jk as seen from within grain j. For use below we note that, as a consequence of this notation, we have

$$\mathbf{n}_{jk} = -\mathbf{n}_{kj} \tag{5}$$

everywhere on the grain boundary G_{jk}.

Next, we consider the sum of expressions such as Eq. (4) over all grains:

$$\sum_{j,k} \int_{\mathsf{G}_{jk}} \mathbf{u}_{\mathsf{G}_{jk}} \otimes \mathbf{n}_{jk} \mathrm{d}A + \sum_j \int_{\mathsf{S}_\mathsf{j}} \mathbf{u}_{\mathsf{S}_j} \otimes \mathbf{n}_j \mathrm{d}A = \sum_j \int_{\mathsf{C}_j} \nabla \mathbf{u} \mathrm{d}V \,. \tag{6}$$

Each grain boundary is counted twice in this sum, once as G_{jk} and once as G_{kj}. It is convenient to introduce a new notation were boundaries – labelled by l – are counted only once. Furthermore, we account for Eq. (5) and we further simplify Eq. (6) by noting that the summation over the S_j gives S and the summation over the C_j gives B. We thus obtain

$$\sum_l \int_{\mathsf{G}_l} -[\mathbf{u}]_{\mathsf{G}_l} \otimes \mathbf{n}_l \mathrm{d}A + \int_{\mathsf{S}} \mathbf{u}_{\mathsf{S}} \otimes \mathbf{n} \mathrm{d}A = \int_{\mathsf{B}} \nabla \mathbf{u} \mathrm{d}V \tag{7}$$

with the following notation: Let G_l denote the grain boundary denoted by G_{jk} and G_{jk} in our earlier notation.

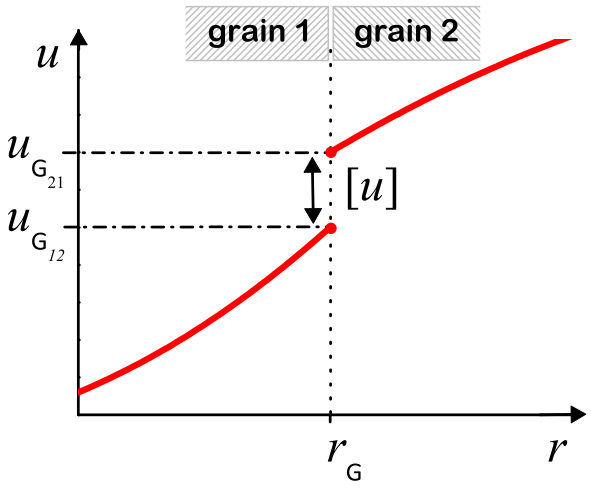

FIG. 3. Schematic illustration of the variation of displacement, u, (solid graph) with position, r, in the vicinity of a grain boundary. The terms $u_{\mathsf{G}_{12}}$ and $u_{\mathsf{G}_{21}}$ denote the limiting value of the displacement as the boundary–located at position r_G–is approached from within grains 1 and 2, respectively. The displacement jump is denoted by $[u]$.

Without lack of generality we orient that grain boundary by setting $\mathbf{n}_l$ as the outward normal as seen from grain j. In other words, $\mathbf{n}_l = \mathbf{n}_{jk}$. Then

$$[\mathbf{u}]_{\mathsf{G}_l}(\mathbf{r}_{\mathsf{G}_l}) = \mathbf{u}_{\mathsf{G}_{kj}}(\mathbf{r}_{\mathsf{G}_l}) - \mathbf{u}_{\mathsf{G}_{jk}}(\mathbf{r}_{\mathsf{G}_l}) \tag{8}$$

is the *displacement jump* across G_l at position $\mathbf{r}_{\mathsf{G}_l}$ on G_l.

Jumps in the displacement at the grain boundaries are a central concept in our theory. They embody the fact that the limiting values of $\mathbf{u}$ at position $\mathbf{r}_{\mathsf{G}_l}$ on G_l differ depending on whether $\mathbf{r}$ is approached from within crystallite C_j or from its neighbor, crystallite C_k. This is illustrated in Fig. 3.

Figure 4 reproduces a graph from Ref. [23] that illustrates the decomposition of $[\mathbf{u}]$ into a normal part and a tangential part:

$$[\mathbf{u}] = \boldsymbol{\tau} + \varepsilon \mathbf{n} \,. \tag{9}$$

The magnitude, ε, of the normal part of $[\mathbf{u}]$ represents the *stretch*, a change in grain boundary excess free volume by deformation of the matter in the grain boundary core along the boundary normal. The tangential component, $\boldsymbol{\tau}$, of $[\mathbf{u}]$ is the *slip* of Ref.[23], a vector that quantifies the local magnitude and direction of grain boundary sliding.

In an atomistic description of grain boundary deformation one wishes to distinguish the regimes of elastic and plastic deformation. With regard to tangential deformation, we may admit an excess shear compliance at the boundary in the elastic regime. This deformation

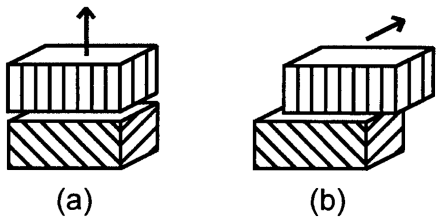

FIG. 4. Schematic illustration of the interfacial deformation modes stretch (a) and slip (b) that give rise to displacement jumps.

mode would break no interatomic bonds and it might entail a reversible (*e.g.*, linear) variation of slip with stress. By contrast, plastic deformation–in other words, grain boundary sliding–may change the interatomic coordination and will not generally display a reversible slip-stress law. Our continuum description in terms of displacement jumps does not discriminate between the two types of atomic-level processes. Small ('elastic') and large ('plastic') shear events both map into a jump discontinuity of the displacement field. Thus, we use the term 'slip' equally for both types of processes.

C. Grain boundary discontinuity tensor

When searching for a parameter that describes the local deformation at grain boundaries in the context of polycrystal deformation, one notes that the sign of $[\mathbf{u}]_{\mathsf{G}_l}$ depends on the orientation of the normal, outward as seen from grain j or outward as seen from grain k. Since that orientation can be chosen arbitrarily, $[\mathbf{u}]_{\mathsf{G}_l}$ alone is not a useful variable for grain boundary deformation. However, one can readily verify that the quantities $[\mathbf{u}]_{\mathsf{G}_l} \otimes \mathbf{n}_l$ are invariant with respect to choice of the orientation of the normal. Here, we find it useful to describe the displacement jump in terms of the *discontinuity tensor*, which we introduce as

$$\mathbb{D}_l = \frac{1}{2}\left([\mathbf{u}]_{\mathsf{G}_l} \otimes \mathbf{n}_l + \mathbf{n}_l \otimes [\mathbf{u}]_{\mathsf{G}_l}\right) . \tag{10}$$

By using the identities given in the Appendix, one obtains useful results for $\mathbb{D}$. Let us first note that the displacement jump can be decomposed into slip and stretch through

$$\boldsymbol{\tau} = \mathbb{P}\cdot[\mathbf{u}] \quad , \quad \varepsilon = \mathbf{n}\cdot[\mathbf{u}] , \tag{11}$$

where $\mathbb{P}$ denotes the projection tensor for the grain boundary plane (*cf.* Appendix). The equivalent relations, which retrieve slip and stretch from $\mathbb{D}$, are

$$\boldsymbol{\tau} = 2\mathbb{P}\cdot\mathbb{D}\cdot\mathbf{n} \quad , \quad \varepsilon = \mathrm{tr}(\mathbb{D}) . \tag{12}$$

Along with Eqs. (3) and (7), the definition of $\mathbb{D}$ (Eq. (10)) suggests that the macroscopic strain depends on $\mathbb{D}$ via

$$\mathbf{E}_{\mathrm{eff}} = \frac{1}{V_{\mathsf{B}}}\left(\int_{\mathsf{B}} \mathbf{E}\mathrm{d}V + \sum_l \int_{\mathsf{G}_l} \mathbb{D}\mathrm{d}A\right) . \tag{13}$$

Conceptually, we may want to think of the individual grain boundary sliding and stretching events as rigid body displacements of the neighboring grains relative to each other. This concept can be reconciled with the nonuniform nature of the displacement jump when we re-write Eq. (13) in terms of averages:

$$\mathbf{E}_{\mathrm{eff}} = \langle\mathbf{E}\rangle_{\mathsf{B}} + \frac{1}{V_{\mathsf{B}}}\sum_l A_l\langle\mathbb{D}\rangle_{\mathsf{G}_l} . \tag{14}$$

The averages $\langle\mathbb{D}\rangle_{\mathsf{G}_l}$ in that equation reduce to exact values of the discontinuity tensor in the limit where the displacement jump is uniform on a planar boundary l, as in rigid body sliding.

A special case of Eq. (14), which describes the contribution of stretch to the net volume change, is obtained by taking the trace of the equation and by accounting for the fact that $\mathrm{tr}(\mathbf{E}) = \Delta V/V$ in the bulk along with Eq. (12) for the grain boundaries:

$$\Delta V = V_{\mathsf{B}}\langle\mathrm{tr}(\mathbf{E})\rangle_{\mathsf{B}} + \sum_l A_l\langle\varepsilon\rangle_{\mathsf{G}_l} . \tag{15}$$

This embodies the additivity of the volume changes in the bulk and at the interfaces.

III. STRESS AND MECHANICAL EQUILIBRIUM

Deformation by grain boundary sliding leads to incompatibilities at triple junctions that need to be removed by crystal plasticity or by elastic deformation. As we shall find in this Section, the strain fields associated with elastic accommodation do not contribute significantly to the overall macroscopic strain. This follows from a balance of stress law that will now be derived.

A. External work of deformation

We start out by analyzing the total *external* mechanical work of deformation, which is the work done against the traction force field, $\mathbf{t}(\mathbf{x}_{\mathsf{S}})$, on the surface:

$$\delta W_{\mathrm{ext}} = \int_{\mathsf{S}} \delta\mathbf{u}\cdot\mathbf{t}\mathrm{d}A . \tag{16}$$

Let us restrict attention to traction that can be generated from a uniform effective external stress, $\mathbf{t}(\mathbf{x}) = \mathbf{S}_{\mathrm{ext}}\cdot\mathbf{n}(\mathbf{x})$ with $\mathbf{S}_{\mathrm{ext}}$ a symmetric second rank tensor. For instance, $\mathbf{S}_{\mathrm{ext}}$ may represent the uniaxial stress in an experimental tension or compression test. Then, using Eq. (7), along

with Eq. (A1) from the Appendix, Eq. (16) can be re-expressed as

$$\delta W_{\rm ext} = \mathbf{S}_{\rm ext} : \int_{\mathsf{S}_l} (\delta\mathbf{u}\otimes\mathbf{n})\mathrm{d}A = \mathbf{S}_{\rm ext} : \left(\sum_l \int_{\mathsf{G}_l} [\mathbf{u}]_{\mathsf{G}_l}\otimes\mathbf{n}_l \mathrm{d}A + \int_{\mathsf{B}} \nabla\mathbf{u}\mathrm{d}V \right) . \quad (17)$$

Since we took $\mathbf{S}_{\rm ext}$ as symmetric, we may equivalently write

$$\delta W_{\rm ext} = \mathbf{S}_{\rm ext} : \sum_l \int_{\mathsf{G}_l} \mathbb{D}_{\mathsf{G}_l}\mathrm{d}A + \mathbf{S}_{\rm ext} : \int_{\mathsf{B}} \mathbf{E}\mathrm{d}V \ . \quad (18)$$

B. Constitutive equations and local equilibrium conditions

In order to introduce the notion of internal stress, consider free energy densities Ψ (per volume) and ψ (per area) for bulk and surface or interface, respectively, so that the net free energy of a body B with surface S and internal interfaces G_l is

$$\delta\mathcal{F} = \int_{\mathsf{B}} \Psi\mathrm{d}V + \int_{\mathsf{S}} \psi\mathrm{d}A + \sum_l \int_{\mathsf{G}_l} \psi\mathrm{d}A \ . \quad (19)$$

Gurtin et al. [23] have shown that appropriate constitutive equations for solids with 'deformable' interfaces – where displacement jumps are permitted – are $\Psi = \Psi(\mathbf{E},\mathbf{r})$ and $\psi = \psi(\mathbb{E},\mathbb{H},[\mathbf{u}],\mathbf{r}_{\mathsf{S}})$. The mean tangential strain, $\mathbb{E}$, and the relative displacement gradient, $\mathbb{H}$, are defined as follows: Let $\mathbf{E}_{\mathsf{G}_{jk}}$ and $\nabla\mathbf{u}_{\mathsf{G}_{jk}}$ be the limits of $\mathbf{E}$ and of $\nabla\mathbf{u}$ as the boundary between grains j and k is approached from inside grain j. Then

$$\mathbb{E} = \frac{1}{2}\mathbb{P}(\mathbf{E}_{\mathsf{G}_{jk}} + \mathbf{E}_{\mathsf{G}_{kj}})\mathbb{P} \ . \quad (20)$$

$$\mathbb{H} = \left(\nabla\mathbf{u}_{\mathsf{G}_{jk}} - \nabla\mathbf{u}_{\mathsf{G}_{kj}}\right)\mathbb{P} \ . \quad (21)$$

Furthermore [23],

$$\mathrm{d}\Psi = \mathbf{S} : \mathrm{d}\mathbf{E} \ , \ \mathrm{d}\psi = \mathbb{S} : \mathrm{d}\mathbb{E} + \mathbb{K} : \mathrm{d}\mathbb{H} + \mathbf{s}\cdot\mathrm{d}[\mathbf{u}] \ , \quad (22)$$

where $\mathbf{S}$, $\mathbb{S}$, $\mathbb{K}$, and $\mathbf{s}$ denote the bulk stress tensor, two surface stress tensors, and a vector quantity that is energy-conjugate to $[\mathbf{u}]$. For use below we note that, since $\mathbb{S}$ and $\mathbb{E}$ are tangential superficial tensors, it follows that [23]

$$\mathbb{S} : \mathrm{d}\mathbb{E} = \mathbb{S} : \mathrm{d}\mathbf{E} \ . \quad (23)$$

The relevant equilibrium conditions are [23]

$$\mathrm{div}\mathbf{S} = 0 \quad (24)$$

for the bulk, along with the two relations for the interface,

$$[\mathbf{S}\mathbf{n}] + \mathrm{div}_{\mathrm{S}}\mathbb{S} = 0 \quad (25)$$

and

$$\langle\mathbf{S}\rangle\mathbf{n} + \mathrm{div}_{\mathrm{S}}\mathbb{K} - \mathbf{s} = 0 \ . \quad (26)$$

By $\mathrm{div}_{\mathrm{S}}$ we denote the surface divergence operator on G; $\langle\mathbf{S}\rangle$ refers to the mean of the limiting values of the bulk stress tensors on the two sides of the interface.

The surface stress $\mathbb{S}$ represents the tendency of a surface or of an internal interface to compress or expand the bulk crystal lattice. This quantity has been well studied for free surfaces [24, 25], and first results for grain boundaries are available [26, 27]. A second surface stress, $\mathbb{K}$, relates to a dependency of the the superficial free energy density on differences in the strain in the two crystals abutting at the common interface. While this phenomenon has been discussed since early work by Herring [28], few data from experiment or atomistic simulation has been forthcoming [29–31]. The paucity of data for $\mathbb{K}$ indicates that the quantity is of little relevance for real materials under presently accessible experimental conditions. In the following, we shall neglect the dependency of ψ on $\mathbb{H}$. More precisely, we shall take $\mathrm{div}_{\mathsf{G}}\mathbb{K}$ as negligible. This approximation is improved when $\mathbb{K}$ is small and/or the grain boundaries have a small curvature. Then, Eq. (26) simplifies to

$$\langle\mathbf{S}\rangle\mathbf{n} = \mathbf{s} \ . \quad (27)$$

At this point it is noted that, at any given position in the interface (*cf.* Eq. (A1)),

$$\mathbf{s}\cdot\mathrm{d}[\mathbf{u}] = (\langle\mathbf{S}\rangle\mathbf{n})\cdot\mathrm{d}[\mathbf{u}] = \langle\mathbf{S}\rangle : \mathrm{d}\mathbb{D} \ . \quad (28)$$

This implies that the superficial free energy density may here be taken as $\psi = \psi(\mathbb{E},\mathbb{D})$, with

$$\delta\psi = \mathbb{S} : \delta\mathbb{E} + \langle\mathbf{S}\rangle : \delta\mathbb{D} \ . \quad (29)$$

In other words, the energy-conjugate quantity to the discontinuity tensor is the mean of the bulk stresses on the two sides of the interface.

So far, the considerations in this subsection were focussed on internal interfaces. At the external surface, we do not consider displacement jumps. We may then describe the superficial energy by the function $\psi(\mathbb{E},\mathbf{r}_{\mathsf{S}})$ with $\mathrm{d}\psi = \mathbb{S}\mathrm{d}\mathbb{E}$.

C. Balance law

In terms of the above definitions, a variational statement for the change, $\delta\mathcal{F}$, of the net free energy (in other words, the *reversible* part of the work of deformation) is

$$\delta\mathcal{F} = \int_{\mathsf{B}} \mathbf{S} : \delta\mathbf{E}\mathrm{d}V + \int_{\mathsf{S}} \mathbb{S} : \delta\mathbb{E}\mathrm{d}A + \sum_l \int_{\mathsf{G}_l} \left(\mathbb{S} : \delta\mathbb{E} + \langle\mathbf{S}\rangle : \delta\mathbb{D}\right)\mathrm{d}A \ . \quad (30)$$

with the equilibrium condition

$$\delta\mathcal{F} - \delta W_{\rm ext} = 0. \quad (31)$$

By substituting Eqs. (17), (30) and (27), and accounting for Eq. (23), Eq. (31) is converted into

$$0 = \int_{\mathsf{B}} (\mathbf{S} - \mathbf{S}_{\text{ext}}) : \delta\mathbf{E}\,\mathrm{d}V + \int_{\mathsf{S}} \mathbb{S} : \delta\mathbf{E}\,\mathrm{d}A + \sum_l \int_{\mathsf{G}_l} (\mathbb{S} : \delta\mathbf{E} + (\langle\mathbf{S}\rangle - \mathbf{S}_{\text{ext}}) : \delta\mathbb{D})\,\mathrm{d}A \,. \quad (32)$$

At equilibrium, this statement must hold for arbitrary deformation fields and, therefore, in particular for all smooth displacement fields that represent uniform strains $\delta\mathbf{E}_0$ and vanishing displacement jump. Here, Eq. (32) takes on the simple form

$$0 = \int_{\mathsf{B}} (\mathbf{S} - \mathbf{S}_{\text{ext}})\,\mathrm{d}V : \delta\mathbf{E}_0 + \int_{\mathsf{S}} \mathbb{S}\mathrm{d}A : \delta\mathbf{E}_0 + \sum_l \int_{\mathsf{G}_l} \mathbb{S}\mathrm{d}A : \delta\mathbf{E}_0 \,. \quad (33)$$

Since this condition must hold for arbitrary values of $\delta\mathbf{E}_0$, it follows that

$$0 = \int_{\mathsf{B}} (\mathbf{S} - \mathbf{S}_{\text{ext}})\,\mathrm{d}V + \int_{\mathsf{S}} \mathbb{S}\mathrm{d}A + \sum_l \int_{\mathsf{G}_l} \mathbb{S}\mathrm{d}A \,. \quad (34)$$

Equation (33) is a generalization of the capillary equation for solids from Ref. [32] to solids with interfaces that can suffer displacement jumps and to nonhydrostatic external load. The important message is that the balance equation continues to hold even when the interfaces exhibit the extra degree of freedom of stretch and slip. It is emphasized that empirical values of $\mathbb{S}$ are such that the surface stress term has a significant impact exclusively for materials which are extremely small-grained, with grain sizes well below 10 nm [26, 27]. Thus, the mean stress in the bulk is simply governed by the external stress. For a linear elastic material, this means that the mean strain in the bulk is also governed by $\mathbf{S}_{\text{ext}}$. In other words, the stress- and strain fields that are prompted by elastic accommodation will not significantly contribute to the macroscopic strain.

In response to changes of the external load, solids will typically undergo transient or sustained *plastic* deformation, including grain boundary sliding and stretch. The material is then not at equilibrium. Yet, since mechanical equilibrium is established at the speed of sound, Eq. (33) will hold to reasonable approximation unless the deformation is extremely fast. Her again, we conclude that stress and strain from elastic accommodation represent internal heterogeneities that do not contribute significantly to the macroscopic deformation.

IV. RELATION TO DISLOCATION PLASTICITY

Dislocation plasticity is readily incorporated into our analysis. We have considered grain boundary sliding and stretching in terms of relative displacements of the two crystals abutting on a grain boundary. Similarly, the movement of a dislocation displaces the regions of crystal on the two adjacent sides of the glide or climb plane by the Burgers vector, $\mathbf{b}$. This process leaves behind a surface which is not necessarily a lattice defect but which exhibits a displacement jump, $[\mathbf{u}] = -\mathbf{b}$ [33, 34].

To quantify the above notion of dislocation plasticity, consider a straight segment D_m of a dislocation which is characterized by the Burgers vector $\mathbf{b}_m$ and the line vector $\mathbf{l}_m$ [34]. We take the line vector as parallel to the line and of magnitude equal to the line length. When D_m moves by the distance $\delta\mathbf{s}$ normal to $\mathbf{l}_m$, then a displacement jump of value $\mathbf{b}_l$ is left behind in the plane containing $\mathbf{l}_m$ and $\delta\mathbf{s}$. The area swept by the dislocation in that plane is obtained as the magnitude, δA_m, of the vector

$$\delta\mathbf{A}_m = \mathbf{l}_m \times \delta\mathbf{s} \,. \quad (35)$$

The normal to the plane is the unit vector along $\delta\mathbf{A}_m$. This implies that the contribution, $\mathbb{D}_m\delta A_m$, of the local deformation event in question to the net deformation can be expressed as

$$\mathbb{D}_m\delta A_m = \frac{1}{2}\left(\mathbf{b}_m \otimes (\mathbf{l}_m \times \delta\mathbf{s}) + (\mathbf{l}_m \times \delta\mathbf{s}) \otimes \mathbf{b}_m\right) \,. \quad (36)$$

In order to obtain the net deformation due to all glide and climb events of all dislocation segments, we sum over all segments:

$$\delta\mathbf{E}^{\text{dis}}_{\text{eff}} = \frac{1}{V_{\mathsf{B}}} \sum_m \mathbb{D}_m\delta A_m \,. \quad (37)$$

This equation is formally similar to Eq. (14). In the general case of simultaneous deformation by bulk elasticity, grain boundary processes, and bulk dislocation plasticity the right-hand side terms of both equations are additive.

As a consistency check one can verify (Appendix B) that the work done by an external stress against the strain $\delta\mathbf{E}^{\text{dis}}_{\text{eff}}$ in Eq. (37) agrees with the work done against the Peach-Köhler forces.

V. A TOY MODEL FOR THE EFFECTIVE ELASTIC RESPONSE OF NANOCRYSTALLINE SOLIDS

A. Model

In this section we present an example for the application of our theory to the deformation of nanocystalline materials. In an attempt to discuss the ramifications of grain boundary deformation for the effective macroscopic *elastic* response, we investigate one of the simplest conceivable models of grain boundary excess elasticity. To set the stage, we recall that 78 independent excess elastic parameters can be identified for a linear elastic and otherwise general deformable grain boundary [23]. Each of these parameters may depend on the five crystallographic

degrees of freedom of the boundary. It therefore appears futile to attempt an experimental study of the complete parameter space of grain boundary elasticity.

Among the various excess elastic constants, previous studies of the impact of interfacial elasticity on the effective macroscopic elastic response of materials (*cf.* Ref. [36] and references therein) have focused on only two, which describe the response of the surface stress $\mathbb{S}$ to the mean bulk strain $\mathbb{E}$ at the interface. The parameters in question, the surface excess Lamé constants λ_S and μ_S, were first defined more than three decades ago by Gurtin and Murdoch [35] in their discussion of free surfaces. Yet, there is so far no established experimental data base for λ_S and μ_S in any material. This sheds doubt on the experimental significance of models of solid-solid interfaces which focus on surface stress and ignore the discontinuity tensor. In fact, atomistic studies point at a different picture [8–10]. These studies highlight in-plane shear softening as the dominant characteristics of grain boundary local elastic behavior. The observation suggests that a simple model may focus on the response of slip to projected shear stress in the boundary plane.

With the above considerations in mind, we inspect a toy model in which the excess elasticity of the grain boundary is reduced to the following form:

$$[\mathbf{u}] = k\mathbf{t} \ , \tag{38}$$

with

$$\mathbf{t} = \mathbb{P} \cdot (\langle \mathbf{S} \rangle \cdot \mathbf{n}) \ , \tag{39}$$

the projected mean shear traction in the boundary plane and k a scalar slip compliance parameter. The deformation mode comprises slip only, no stretch, and it is thus volume-conserving. Furthermore, grain boundaries are modeled here as isotropic in the plane. The implication is that grain boundaries slip in the direction of the largest projected shear stress and by a distance that is proportional to that stress.

In order to further simplify the discussion of the macroscopic elastic response of the polycrystalline solid, let us assume that, on average, the local values of $\mathbf{S}$ and k along the grain boundary network are not systematically correlated to each other or to the orientation of the grain boundary normal in space. We can then take $\langle \mathbf{S} \rangle = \mathbf{S}_{\text{ext}}$ in Eq. (39) and derive the excess deformation by averaging the discontinuity which ensues from Eq. (38) tensor over all grain boundary orientations.

Here, as in other instances where the local stress or strain are correlated with the orientation of the surface or interface normal [32, 38], it is profitable to represent the microstructural anisotropy through the interface orientation distribution function [39], $G(\theta, \varphi)$. With the orientation of $\mathbf{n}$ parameterized by the inclination (or colatitude), φ, and by the longitude, θ, the function $G(\varphi, \theta)$ is defined so that–within the volume V_B–the area of all segments of grain boundary with orientation between (φ, θ) and $(\varphi + \delta\varphi, \theta + \delta\theta)$ is given by $\delta A = V_B G(\varphi, \theta) \sin\varphi \delta\theta \delta\varphi$.

In terms of G, the integration in position space in expressions such as Eq. (13) can be converted into one in orientation space, so that the contribution of the grain boundary slip compliance to the macroscopic strain is obtained as

$$\begin{aligned} \mathbf{E}^{\text{slip}} &= \frac{1}{V_B} \int_G \mathbb{D}(\mathbf{x}) \mathrm{d}A \\ &= \int_\Omega \mathbb{D}(\varphi, \theta) G(\varphi, \theta) \sin\varphi \mathrm{d}\theta \mathrm{d}\varphi \ . \end{aligned} \tag{40}$$

In general, the grain boundary orientation distribution function can be anisotropic, for instance for the columnar grain geometries typically found in vapor-deposited thin films or for lamellar microstructures produced by rolling. For simplicity, we here consider the case of an isotropic grain geometry. Here, the orientation distribution function is a constant, $G(\varphi, \psi) = \alpha$, with $\alpha = A/V_B$ the volume-specific grain boundary area.

As two specific stress states we consider a uniaxial stress and a pure shear stress. For an orthonormal basis, they can be expressed in matrix form as

$$\mathbf{S_1} = \begin{pmatrix} 0 & 0 & 0 \\ 0 & 0 & 0 \\ 0 & 0 & S_1 \end{pmatrix}, \tag{41}$$

$$\mathbf{S_2} = \begin{pmatrix} 0 & 0 & 0 \\ 0 & 0 & S_2 \\ 0 & S_2 & 0 \end{pmatrix}. \tag{42}$$

By means of illustration, let us evaluate the explicit form of $\mathbb{D}(\varphi, \psi)$ for the uniaxial stress $\mathbf{S_1}$. Taking $\mathbf{n} = (\cos\theta \sin\varphi, \sin\theta \sin\varphi, \cos\varphi)$, and accounting for Eqs. (10) and 38, we obtain

$$\mathbb{D} = -kS_1 \begin{pmatrix} \cos^2\theta \cos^2\varphi \sin^2\varphi & \cos\theta \sin\theta \cos^2\varphi \sin^2\varphi & \frac{1}{8}\cos\theta \sin 4\varphi \\ \cos\theta \sin\theta \cos^2\varphi \sin^2\varphi & \sin^2\theta \cos^2\varphi \sin^2\varphi & \frac{1}{8}\sin\theta \sin 4\varphi \\ \frac{1}{8}\cos\theta \sin 4\varphi & \frac{1}{8}\sin\theta \sin 4\varphi & -\cos^2\varphi \sin^2\varphi \end{pmatrix}. \tag{43}$$

Using this type of expression with Eq. (40), and adding the bulk elastic response, the net effective strains for uniaxial stress and for pure shear are obtained, respectively, as

$$\mathbf{E}_{\mathbf{1}}^{\text{eff}} = \frac{S_1}{Y_0} \begin{pmatrix} -\nu_0 & 0 & 0 \\ 0 & -\nu_0 & 0 \\ 0 & 0 & 1 \end{pmatrix} + \frac{2kS_1\alpha}{15} \begin{pmatrix} -\frac{1}{2} & 0 & 0 \\ 0 & -\frac{1}{2} & 0 \\ 0 & 0 & 1 \end{pmatrix}, \tag{44}$$

$$\mathbf{E}_{\mathbf{2}}^{\text{eff}} = \left(\frac{S_2}{2G_0} + \frac{kS_2\alpha}{5} \right) \begin{pmatrix} 0 & 0 & 0 \\ 0 & 0 & 1 \\ 0 & 1 & 0 \end{pmatrix}, \tag{45}$$

where Y_0, G_0, and ν_0 denote the Young modulus, shear modulus and Poisson number, respectively, of the bulk solid.

It is also of interest to compute the root-mean square slip magnitudes, $\overline{\tau}$. For the two loading modes these are obtained, respectively, as

$$\overline{\tau}_1 = \sqrt{\frac{2}{15}} k S_1 \quad , \quad \overline{\tau}_2 = \sqrt{\frac{2}{5}} k S_2 \, . \tag{46}$$

This means that the extra strains can simply be written as

$$\mathbf{E}_{\mathbf{1}}^{\mathrm{slip}} = \sqrt{\frac{6}{5}} \frac{\tau_1}{L} \begin{pmatrix} -\frac{1}{2} & 0 & 0 \\ 0 & -\frac{1}{2} & 0 \\ 0 & 0 & 1 \end{pmatrix} , \tag{47}$$

$$\mathbf{E}_{\mathbf{2}}^{\mathrm{slip}} = \frac{3}{\sqrt{10}} \frac{\tau_2}{L} \begin{pmatrix} 0 & 0 & 0 \\ 0 & 0 & 1 \\ 0 & 1 & 0 \end{pmatrix} , \tag{48}$$

Since the numerical factors are close to unity, the two last equations agree closely with what is found for the brick model of Fig. 1. In Eq. (47) we have used the relation between the grain size, L, and the specific grain boundary area, $L = 3/\alpha$ for idealized grains with a spherical shape.

Let us now present the resulting equations for the effective values of Y, G, and ν:

$$Y^{\mathrm{eff}} = \frac{15 Y_0}{15 + 2 k Y_0 \alpha} \approx Y_0 \left(1 - \frac{2}{15} k Y_0 \alpha \right) \tag{49}$$

$$G^{\mathrm{eff}} = \frac{5 G_0}{5 + 2 k G_0 \alpha} \approx G_0 \left(1 - \frac{2}{5} k G_0 \alpha \right) \tag{50}$$

$$\nu^{\mathrm{eff}} = \frac{15\nu_0 + k Y_0 \alpha}{15 + 2 k Y_0 \alpha} \approx \nu_0 + \frac{1}{15} k Y_0 \alpha \, (1 - 2\nu_0) \tag{51}$$

where the terms on the very right-hand side are series expansions around $\alpha = 0$ to first order in α.

As an insight from the toy model, we advertise that Eq. (44) attributes a Poisson ratio $\nu^{\mathrm{slip}} = 1/2$ to the extra strain due to grain boundary slip. This is not surprising, since the neglect of stretch in our toy model implies that we consider a volume-conserving deformation mode. Since the bulk deformation of real materials has $\nu_0 < 1/2$, the model thus implies that slip-controlled grain boundary deformation brings an increase in Poisson ratio with decreasing grain size. The same reasoning also implies that the effective bulk modulus, K^{eff}, is here independent of the grain size,

$$K^{\mathrm{eff}} = K_0 \, . \tag{52}$$

These simple observations may be checked against experimental data for the size-dependent elastic moduli of nanocystalline metals. Such data has recently been reported by Grewer et al. for nanocrystalline Pd, Ref. [7]. We shall now inspect their results in the light of our model.

B. Comparison to experiments with nanocystalline Palladium

The data in Ref. [7] was obtained with materials prepared by in-situ consolidation of nanoscale clusters in an ultrahigh vacuum environment (inert-gas condensation technique, igc). In that study, the effective elastic constants of the bulk samples were determined by an ultrasound pulse-echo method. This was done in-situ in an x-ray powder diffractometer, with the grain size determined from the Bragg reflection broadening. The experiment took several days, while the microstructure was evolving by room-temperature grain growth.

Nanocrystalline Pd prepared by igc may be approximated as an isotropic material, free of crystallographic texture and with an isotropic grain boundary orientation distribution function [7]. The effective macroscopic elastic response is therefore represented by two independent elastic parameters, for instance any pair of values chosen from Y^{eff}, G^{eff}, K^{eff}, and ν^{eff}. As its data base, the experiment in Ref. [7] exploits the longitudinal and transverse sound velocities at each grain size. The established equations for the sound velocity in elastically isotropic continua afford a computation of the effective macroscopic elastic constants. Here we use this data for comparison to our model, and we ignore the decomposition into bulk and interface elastic behavior of Ref. [7]. Compared to the present approach, the decomposition in Ref. [7] rests on a different description, which models interfaces as three-dimensional slabs of material with independent bulk elastic constants, *cf.* for instance Ref. [37]. Much can be said for and against each of the two approaches, but we here dwell on a description of interfaces in terms of a two-dimensional manifold if only due to the natural incorporation of the anisotropy of the in-plane (sliding) and out-of-plane (stretch) deformation behavior.

Figure 5 shows the effective elastic constants Y^{eff}, G^{eff}, K^{eff}, and ν^{eff} that are obtained from the experimental ultrasound data of Ref. [7] [40]. It is immediately obvious that the bulk modulus is indeed much less dependent on grain size than the remaining parameters, as predicted by the model of Section V A. It is also seen that the prediction of an increase in Poisson ratio at small size is indeed born out by the data. This suggests that the toy model catches essential characteristics of the grain boundary elastic response and of its impact on the effective elasticity of nanoscale solids.

For not too large α, all elastic parameters vary linearly with α. We have fitted the data points in the interval of linear behavior, $\alpha < 0.33\mathrm{nm}^{-1}$, by straight lines. The coefficients from these four independent straight-line fits are given in Table 1. The extrapolation to $\alpha = 0$ provides bulk elastic parameters Y_0, G_0, K_0 and ν_0 in good agreement with reported values.

In order to test the toy model, we have performed a second fit procedure. Here, the data for the α-dependece of the experimental effective elastic parameters is fitted

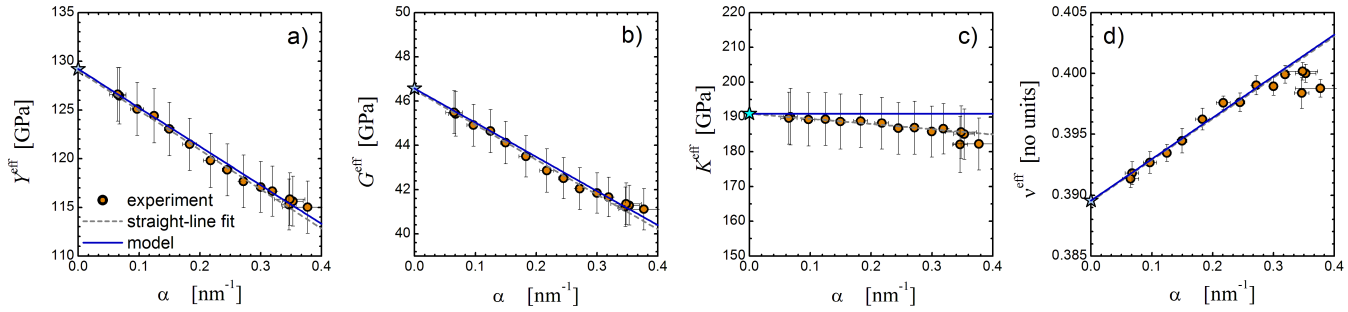

FIG. 5. Effective macroscopic elastic constants of nanocrystalline Pd, plotted versus the volume-specific grain boundary area, α. $Y^{\rm eff}$, $G^{\rm eff}$, $K^{\rm eff}$, and $\nu^{\rm eff}$ denote the effective Youngs modulus, shear modulus, bulk modulus and Poisson number, respectively. Circles, experimental data from the study in Ref. [7] [40]. Dashed lines, best straight-line fit to the experiment in the interval of linear behavior, $0.066{\rm nm}^{-1} < \alpha < 0.33{\rm nm}^{-1}$. Solid lines, fit with the linearized variant of Eqs. (49-51), using the ordinate intercepts of the straight-line fits (asterisks) for the values of the bulk elastic constants and using the sliding compliance, k, as the single adjustable parameter. The identical value, k = 18.0 pm/GPa, is used to fit all three elastic constants. Note the excellent agreement, supporting the model of an excess compliance that is exclusively due to grain boundary sliding deformation.

TABLE I. Elastic constants and dependence on the specific grain boundary area, α. X_0 and $\partial X^{\rm eff}/\partial\alpha|_{\rm exp}$ are the ordinate intercepts and slopes, respectively, of the straight-line fits to the experimental data in Fig. 5. $\partial X^{\rm eff}/\partial\alpha|_{\rm fit}$ denotes the predicted slope based on Eqs. (49-51), using the X_0 from the Table and the value k = 18.0 pm/GPa for the excess sliding compliance, k, as the single adjustable parameter. Note the excellent agreement between the experimental slopes and the value from Eqs. (49-51).

X	X_0	$\partial X^{\rm eff}/\partial\alpha\|_{\rm exp}$	$\partial X^{\rm eff}/\partial\alpha\|_{\rm fit}$
Y	129±2GPa	-41±9 N/m	-40 N/m
G	46.5±0.7 GPa	-16±1 N/m	-16 N/m
K	191±5 GPa	-15±26 N/m	0
ν	0.3895±0.0006	+34±3 pm	+34 pm

by the linearized variant of Eqs. (49-51), using the bulk elastic parameters from the straight-line fits and treating the slip compliance, k, as the single adjustable parameter. The fit is here simultaneous to all four graphs in Fig. 5, with the identical value of k in each case. The excellent agreement (cf. Figure 5 and Table 1) is a nontrivial finding, since two independent elastic parameters are fitted with the single free parameter k. The agreement provides strong support for modeling the excess compliance by a volume-conserving process, such as our toy model of pure slip deformation.

The value of the slip compliance from the fit is k = 18.0 pm/GPa. This implies that a projected shear stress of 1 GPa leads to a slip distance of 18 pm. The exact stress amplitude of the ultrasound experiment is unknown, but it is conservative to assume that it is well below the yield stress of the coarsest-grained samples and thus much smaller than 100 MPa. This implies less than 2pm sliding amplitude. The value is thus less than 1% of an interatomic distance, putting the slip deformation in the experiment well into the elastic regime.

VI. SUMMARY AND CONCLUSIONS

The findings of this study can be summarized as follows:

- Grain boundary slip and grain boundary stretch enter the kinematics of deformation as the tangential and normal part of a displacement jump vector, $[\mathbf{u}]$, that measures the relative displacement of the two crystals abutting at a grain boundary.

- The most relevant quantity for the macroscopic deformation is not $[\mathbf{u}]$ but its Kronecker product, $[\mathbf{u}]\otimes\mathbf{n}$, with the grain boundary normal, $\mathbf{n}$. Furthermore, the impact of the grain-boundary mediated processes on the macroscopic *strain* is governed by the symmetric part of the second rank tensor $[\mathbf{u}]\otimes\mathbf{n}$. We have termed that quantity the *discontinuity tensor*, $\mathbb{D}$.

- The effective macroscopic deformation of a polycrystalline body depends on the local grain boundary deformation via the sum over the mean discontinuity tensors of the boundaries, weighted by the respective grain boundary area. For given magnitudes of $\mathbb{D}$, the macroscopic strain scales with the net grain boundary area per volume or – for equiaxed grain structures – with the inverse grain size.

- In general, grain boundary sliding and stretch lead to incompatibilities of deformation at triple junctions. These incompatibilities require accommodation, for instance by elastic deformation or by dislocation plasticity in the bulk crystal lattices. When the elastic behavior in the bulk is linear, then the relevant elastic deformation does not significantly contribute to the macroscopic strain.

- Dislocation plasticity can be treated in a closely analogous picture. Whereas grain boundary plasticity involves changes, $\delta\mathbb{D}^{\mathrm{gb}}$, in the grain boundary discontinuity tensor on pre-existing internal interfaces of constant area, dislocation plasticity in the bulk crystal lattice involves the generation of new surface suffering a displacement jump that is determined by the constant value, $\mathbb{D}^{\mathrm{dis}}$, of the discontinuity tensor associated with the relevant dislocation event. Thus, conceptually, the net macroscopic strain due to a small change in the deformation variables can be written as

$$\delta\mathbf{E}_{\mathrm{eff}} = \langle\delta\mathbf{E}\rangle_{\mathsf{B}} + \frac{1}{V_{\mathsf{B}}}\sum_l A_l\delta\langle\mathbb{D}^{\mathrm{gb}}\rangle_l + \frac{1}{V_{\mathsf{B}}}\sum_m \mathbb{D}^{\mathrm{dis}}_m\delta A_m \ . \tag{53}$$

- The discontinuity tensor associated with dislocation plasticity in the bulk is the symmetric part of the Kronecker product of Burgers vector, $\mathbf{b}$, and the normal of the glide or climb plane. This latter quantity is parallel to the cross product, $\mathbf{l}\times\delta\mathbf{s}$, of line vector $\mathbf{l}$ and dislocation displacement vector $\delta\mathbf{s}$.

- For reversible processes, the energy-conjugate quantity to the discontinuity tensor can be approximated as the mean, $\langle\mathbf{S}\rangle$, of the bulk stresses on the two sides of the interface. Thus, varying $\mathbb{D}$ *reversibly* changes the interfacial free energy density, ψ, by $\delta\psi \approx \langle\mathbf{S}\rangle : \delta\mathbb{D}$. More generally, $\langle\mathbf{S}\rangle : \delta\mathbb{D}$ measures the total (reversible and irreversible) work of deformation. A similar expression for dislocation plasticity and $\mathbb{D}^{\mathrm{dis}}$ is consistent with the work done against the Peach-Köhler force.

- As an example for the application of our theory to experiment, we have studied a toy model for the elastic response of nanocrystalline materials. Assuming an excess compliance which is dominated by grain boundary slip, we have derived expressions for the variation of the effective macroscopic elastic response with the grain size. The predictions of an increase in Poisson ratio at small size and of essentially constant compressibility compare well to experimental data for nanocrystalline Pd. This supports the conclusion of shear softening at grain boundaries [7] and rules out artifacts from porosity in that study, since pores would increase the compressibility and, therewith, the Poisson ratio.

Since our analysis does not allow for grain boundary migration, the phenomenon of coupled motion (*cf.* the introduction) is not appropriately described here. An extension would incorporate the coupling between the grain boundary slip vector and a displacement of the boundary plane along its normal. Besides the direct contribution of slip to the discontinuity tensor – as treated in our analysis – the boundary migration leads here to an extra contribution to $\mathbb{D}$. We expect that this contribution emerges as the product of jump in the strain tensor at the interface and the volume swept by the segment of boundary when it migrates. However, the analysis is beyond the scope of the present work and awaits a dedicated study.

There are various scenarios in atomistic simulation and experiment that allow the grain-boundary mediated deformation of our analysis to be quantified. Molecular dynamics studies of the mechanical response of nanocrystalline solids to external load supply displacement fields atom by atom. In a suitably coarse-grained description one can determine the limiting values of the displacement fields on both sides of a grain boundary, similar to what is shown in Fig. 3. In principle, this allows the grain boundary sliding and stretch – and, thereby, $\mathbb{D}$ – to be extracted everywhere in the network of grain boundaries. It is also well established that the elastic strain field in the bulk [41] and the net deformation by bulk dislocation activity [6, 21] can be quantified in atomistic simulation, as can the external deformation. Thus, atomistic studies supply all parts of Eq. (53), affording a verification as well as a separate quantification of the individual deformation modes.

In experiment, the grain boundary mediated deformation is most readily accessed when the load is sufficiently small to prevent dislocation activity in the bulk. The bulk deformation is then entirely due to elastic strain. The mean of the bulk elastic strain can be quantified using lattice parameter data from in-situ diffraction experiments [42–46], which can also be combined with macroscopic strain measurement [44, 46]. This is similar to a Simmons-Baluffi [47] type experiment, except that the strain difference is here due to grain boundary deformation rather than vacancy generation. An example is the investigation of different strain measures during hydrogen absorption in nanocrystalline Pd (free of load) [26, 48]. The significant difference in macroscopic strain versus mean lattice strain provides a quantitative measure for the mean stretch due to hydrogen enrichment or depletion in grain boundaries.

In studies of nanomaterial deformation under load, lattice parameter data in the nominally elastic regime is available [42, 44–46]. Deviations between the mean lattice parameter change – which measures the bulk strain – and the macroscopic strain would indicate grain boundary mediated deformation.

In conclusion, therefore, we believe that the contribution of grain boundary slip to the macroscopic deformation of nanocrystalline solids is of sufficient importance to require quantification. The results of the present paper provide a theoretical frame for using results of atomistic simulation or experiment in accomplishing this task.

Acknowledgement: This study was supported by Deutsche Forschungsgemeinschaft (Forschergruppe 714 "Plastizität in Nanomaterialien").

Appendix A: Tensor notation

Let $\mathbf{A}$ denote a symmetric second rank tensor, $\mathbf{B}$ a general second rank tensor, and $\mathbf{c}$, $\mathbf{d}$ vectors. We denote the Kronecker product, an inner product, and the dot product by $\otimes$, : and $\cdot$, respectively. In component notation for an orthonormal basis, $(\mathbf{c}\otimes\mathbf{d})_{ij} = c_i d_j$, $\mathbf{A}:\mathbf{B} = A_{ij}B_{ij}$, $(\mathbf{c}\cdot\mathbf{d}) = c_i d_i$, and $(\mathbf{B}\cdot\mathbf{c})_i = B_{ij}c_j$ with summation convention applied.

The following identities hold:

$$(\mathbf{c}\otimes\mathbf{d}):\mathbf{A} = (\mathbf{d}\otimes\mathbf{c}):\mathbf{A} = \mathbf{c}\cdot\mathbf{A}\cdot\mathbf{d} \tag{A1}$$

and

$$\mathrm{tr}(\mathbf{c}\otimes\mathbf{d}) = \mathbf{c}\cdot\mathbf{d}\,. \tag{A2}$$

Furthermore, with $\mathbf{n}$ a unit vector, $\mathbf{U}$ the unit tensor in three dimensional space, and with $\mathbf{P} = \mathbf{U} - \mathbf{n}\otimes\mathbf{n}$ the projection tensor for the surface with normal $\mathbf{n}$, we have

$$(\mathbf{c}\otimes\mathbf{n})\cdot\mathbf{n} = \mathbf{c}\,, \tag{A3}$$

$$\mathbf{n}\cdot(\mathbf{n}\otimes\mathbf{c})\cdot\mathbf{n} = \mathbf{n}\cdot\mathbf{c}\,, \tag{A4}$$

$$\mathbf{P}\cdot(\mathbf{n}\otimes\mathbf{c})\cdot\mathbf{n} = 0\,. \tag{A5}$$

Appendix B: Peach-Köhler force

Consider a small test volume T which contains dislocation line segments m and which is loaded on its periphery by the uniform stress $\mathbf{S}$. When the dislocations move, the work done against $\mathbf{S}$ is (*cf.* Eq. (18))

$$\delta W = V_{\mathsf{T}}\mathbf{S}:\delta\mathbf{E}_{\mathrm{eff}}\,. \tag{B1}$$

By using first Eq. (37) and then Eq. (36), this expression is transformed into

$$\delta W = \mathbf{S}:\sum_m \mathbb{D}_m\delta A_m \tag{B2}$$

and then

$$\delta W = \mathbf{S}:\frac{1}{2}\sum_m\left[\mathbf{b}_m\otimes(\mathrm{d}\mathbf{l}_m\times\delta\mathbf{s}_m) + (\mathrm{d}\mathbf{l}_m\times\delta\mathbf{s}_m)\otimes\mathbf{b}_m\right]\,. \tag{B3}$$

Since $\mathbf{S}$ is symmetric, we can equivalently write

$$\delta W = \mathbf{S}:\sum_m \mathbf{b}_m\otimes(\mathrm{d}\mathbf{l}_m\times\delta\mathbf{s}_m)\,, \tag{B4}$$

and apply Eq. (A1) to obtain

$$\delta W = \sum_m \mathbf{b}_m\cdot(\mathbf{S}\cdot(\mathrm{d}\mathbf{l}_m\times\delta\mathbf{s}_m))\,. \tag{B5}$$

Equation (B5) agrees with the expression by Peach and Köhler for the work done by the uniform stress $\mathbf{S}$ on a set of moving dislocations [33]. The agreement confirms that the work done against the dislocation discontinuity tensor is identical with the work done against the Peach-Köhler force. This verifies the incorporation of dislocation plasticity into the formalism of the present work.

[1] D. Wolf, V. Yamakov, S.R. Philpot, A. Mukherjee, H. Gleiter, Acta Mater. 53 (2005) 1.
[2] J. Weissmüller, J. Markmann, Adv. Eng. Mater. 7 (2005) 202.
[3] M.A. Meyers, A. Mishra, D.J. Benson, Prog. Mater. Sci. 51 (2006) 427.
[4] J. Markmann, P. Bunzel, H. Rösner, K.W. Liu, K.A. Padmanabhan, R. Birringer, H. Gleiter, J. Weissmüller, Scripta Mater. 49 (2000) 637.
[5] A. Hasnaoui, H. van Swygenhoven, P.M. Derlet, Phys. Rev. B 66 (2002) 184112.
[6] D.V. Bachurin, P. Gumbsch, Acta Mater. 58 (2010) 5491.
[7] M. Grewer, J. Markmann, R. Karos, W. Arnold, R. Birringer, Acta Mater. 59 (2011) 1523.
[8] M.D. Kluge, D. Wolf, J.F. Lutsko, S.R. Philpot, J. Appl. Phys. 67 (1990) 2370.
[9] I. Alber, J.L. Bassani, M. Khantha, V. Vitek, G.J. Wang, Philos. Trans. Roy. Soc. Lond. A 339 (1992) 555.
[10] J. Wang, D. Wolf, S.R. Phillpot, H. Gleiter, Phil. Mag. A 73 (1996) 517.
[11] J.W. Cahn, J.E. Taylor, Acta Mater. 52 (2004) 4887.
[12] J.W. Cahn, Y. Mishin, A. Suzuki, Acta Mater. 54 (2006) 4953.
[13] D.A. Molodov, V.A. Ivanov, G. Gottstein, Acta Mater. 55 (2007) 1843.
[14] A.D. Sheikh-Ali, Acta Mater. 58 (2010) 6249.
[15] A.J. Haslam, D. Moldovan, V. Yamakov, D. Wolf, S.R. Phillpot, H. Gleiter, Acta Mater. 51 (2003) 2097.
[16] D. Farkas, A. Frøseth, H. van Swygenhoven, Scripta Mater. 55 (2006) 695.
[17] H. Rösner, J. Markmann, J. Weissmüller, Philos. Mag. Lett. 84 (2004) 321.
[18] Y.T. Zhu, X.Z. Liao, S.G. Srinivasan, Y.H. Zhao, M.I. Baskes, F. Zhou, E.J. Lavernia, Appl. Phys. Lett. 85 (2004) 5049.
[19] M. Chen, E. Ma, K.J. Hemker, H. Sheng, Y. Wang, X. Cheng, Science 300 (2003) 1275.
[20] A. Frøseth, P.M. Derlet, H. van Swygenhoven, Acta Mater. 52 (2004) 5863.
[21] N.Q. Vo, R.S. Averback, P. Bellon, S. Odunuga, A. Caro, Phys. Rev. B 77 (2008) 134108.
[22] P. Haupt, Continuum Mechanics and Theory of Materials, 2nd. Ed. (Springer, Berlin, 2002).
[23] M.E. Gurtin, J. Weissmüller, F. Larché, Philos. Mag. A 78 (1998) 1093.
[24] H. Ibach, Surf. Sci. Rep. 29 (1997) 193.
[25] R.C. Cammarata, K. Sieradzki, Annu. Rev. Mater. Sci. 24 (1994) 215.
[26] J. Weissmüller, C. Lemier, Phys. Rev. Lett. 82 (1999) 213.

[27] R. Birringer, M. Hoffmann, P. Zimmer, Phys. Rev. Lett. 88 (2000) 206106.
[28] C. Herring, Phys. Rev. 82 (1951) 87.
[29] J.A. Ruud, A. Witvrouw, F. Spaepen, J. Appl. Phys. 74 (1993) 2517.
[30] A.L. Shull, F. Spaepen, J. Appl. Phys. 80 (1996) 6243.
[31] R. Birringer, P. Zimmer, Acta Mater. 57 (2009) 1703.
[32] J. Weissmüller, J. W. Cahn, Acta Mater. 45 (1997) 1899.
[33] M. Peach and J.S. Koehler, Phys. Rev. 80 (1950) 436.
[34] The convention $\mathbf{b} = -[\mathbf{u}]$ reconciles the signs in the definitions of the displacement jump by Gurtin et al. [23] and of the Burgers vector by Peach and Köhler [33]. Furthermore, with $\mathbf{l}$ the line vector, we take $\mathbf{b}$ as closing (from endpoint to startpoint) a *right-handed* (counter-clockwise when $\mathbf{l}$ points towards the observer) Burgers circuit in the deformed solid.
[35] M.E. Gurtin, A.I. Murdoch, Arch. Ration. Mech. Anal. 57 (1975) 291.
[36] H.L. Duan, J. Wang, B.L. Karihaloo, Adv. Appl. Mech. 42 (2008) 1.
[37] Y. Benveniste, T. Miloh, Mechanics Mater. 33 (2001) 309.
[38] Y. Wang, J. Weissmüller, H.L. Duan, J. Mech. Phys. Solids, 58 (2010) 1552.
[39] J.E. Hilliard, Trans. Metall. Soc. AIME 224 (1962) 1201.
[40] Grewer et al. [7] parameterize the mean grain size in terms of an area-weighted mean length, $\langle \ell \rangle_{\mathrm{area}}$, of diffracting columns in their x-ray experiment. By its definition, that parameter is related to the specific grain boundary area via $\alpha = 2/\langle \ell \rangle_{\mathrm{area}}$.
[41] A. Stukowski, J. Markmann, J. Weissmüller, K. Albe, Acta Mater. 57 (2009) 1648.
[42] W. Pantleon, H.F. Poulsen, J. Almer, U. Lienert, Mater. Sci. Eng. A 387-389 (2004) 339.
[43] Z. Budrovic, H. Van Swygenhoven, P.M. Derlet, S. Van Petegem, B. Schmitt, Science 304 (2004) 273.
[44] H. Li, H. Choo, Y. Ren, T.A. Saleh, U. Lienert, P.K. Liaw, F. Ebrahimi, Phys. Rev. Lett. 101 (2008) 015502.
[45] I. Lornadelli, J. Alber, G. Ischia, C. Menapace, A. Molinari, Scripta Mater. 60 (2009) 520.
[46] T. Ulyanenkova, R. Baumbusch, T. Filatova, S. Doyle, A. Castrup, P.A. Gruber, J. Markmann, J. Weissmüller, T. Baumbach, H. Hahn, O. Kraft, Phys. Stat. Sol. A 206 (2009) 1795.
[47] R.O. Simmons, R.W. Balluffi, Phys. Rev. 117 (1960) 52.
[48] C. Lemier, J. Weissmüller, Acta Mater. 55 (2007) 1241.